Frictional properties of anorthite (feldspar): Implications for the lower boundary of the seismogenic zone

Koji Masuda (koji.masuda@aist.go.jp)

Express Letter

Keywords: Fault friction, Feldspar, Anorthite, Albite, Quartz

Posted Date: September 9th, 2020

DOI: https://doi.org/10.21203/rs.3.rs-41023/v2

Version of Record: A version of this preprint was published on September 16th, 2020. See the published version at https://doi.org/10.1186/s40623-020-01271-6.

Abstract

Earthquake magnitude is closely related to the depth extent of the seismogenic zone, and higher magnitude earthquakes occur where the seismogenic zone is thicker. The frictional properties of the dominant mineral constituents of the crust, such as feldspar-group minerals, control the depth extent of the seismogenic zone. Here, the velocity dependence of the steady-state friction of anorthite, the calcic endmember of the feldspar mineral series, was measured at temperatures from 20 to 600 °C, pore pressures of 0 (“dry”) and 50 MPa (“wet”), and an effective pressure of 150 MPa. The results support previous findings that the frictional properties of feldspar play a dominant role in limiting the depth extent of the seismogenic zone. This evidence suggests that brittle deformation of anorthite may be responsible for brittle fault movements in the brittle–plastic transition zone.

Introduction

The depth extent of the part of the crust in which earthquakes occur in a given region (the seismogenic zone) is closely related to the magnitude of the earthquakes that occur in that region. Areas with seismogenic zones with greater depth extents experience larger earthquakes. Knowing the depth extent of the seismogenic zone is therefore important for earthquake hazard planning to mitigate earthquake damage. The processes that cause earthquakes are controlled by the frictional properties of the subsurface rocks in which faults move (e.g., Scholz 1998, 2019). Many laboratory studies have analyzed the velocity dependence of the steady-state friction of gouge consisting, for example, of granite (Blanpied et al. 1991, 1995; Lockner et al. 1986), quartz (Chester and Higgs, 1992), and feldspar (albite) (Masuda et al. 2019), at temperatures and pressures equivalent to those in the seismogenic zone. Blanpied et al. (1995) found that velocity weakening appeared in Westerly granite gouge between 100 and 300 °C under wet conditions. Velocity weakening has been observed in other materials as well in several experiments under wet conditions. To understand the physical mechanisms of deformation processes in the seismogenic zone, a simple deformation model that depends on the material properties of its component materials is useful for obtaining a first approximation of the large-scale seismic behavior of the zone. Chester and Higgs (1992) showed experimentally that the frictional behavior of ultrafine quartz gouge can be understood in terms of a change in the dominant mechanisms of slip. However, there is little published information on the frictional properties of the feldspar group of minerals, which are dominant minerals in the crust. As a result, neither the temperature (depth) dependence of frictional stability for feldspar minerals nor the lower limit of the seismogenic zone are well understood. Masuda et al. (2019) measured the frictional properties of two major mineral components of crustal rocks, quartz and albite (sodic feldspar), under pressure and temperature conditions characteristic of the depths at which earthquakes occur and showed that albite, rather than quartz, was dominant in limiting the depth extent or thickness of the seismogenic zone. Furthermore, seismological observations show a clear correspondence of the lower limit of the seismogenic zone with the 350 to 400 °C isotherm, and this temperature range corresponds better to the transition from brittle deformation to plastic behavior in feldspar than to that in quartz (Hasegawa and Yamamoto 1994).

Feldspars make up 50–60% of the total volume of the Earth's crust. The major feldspar group minerals are albite ($NaAlSi_3O_8$), anorthite ($CaAl_2Si_2O_8$), and K-feldspar ($KAlSi_3O_8$), and anorthite–albite series (plagioclases) are the most abundant minerals in the Earth's crust. Masuda et al. (2019) measured the frictional properties of albite, but those of other plagioclase-series minerals have not yet been measured. In addition, recent investigations of the interface between seismic and aseismic zones have shown that lithological, mechanical, and frictional heterogeneities within the fault zone and the morphology and geometry of the interface significantly affect seismogenic processes (Barnes et al. 2020; Kirkpatrick et al. 2020). Thus, the material properties of the rocks distributed in the lower part of the seismogenic zone can be expected to critically affect seismogenic processes.

In this study, the frictional properties of anorthite, the calcic endmember of the anorthite–albite series, were examined under dry and wet conditions at temperatures from 20 to 600 °C. These results for the frictional behavior of anorthite support previous evidence that feldspar minerals largely determine the depth extent of the seismogenic zone. Moreover, they show that anorthite exhibits brittle behavior under the temperature and pressure conditions of the brittle–plastic transition zone.

Methods

Sliding experiments were conducted in a triaxial gas apparatus in which argon gas was used as the confining medium (Masuda et al. 2002, 2006). A layer of anorthite gouge about 1.0 mm thick was sandwiched between two sawcut alumina cylinders (20 mm in diameter, 40 mm long) in the same configuration as that used by Takahashi et al. (2007, 2011) and Masuda et al. (2019). The anorthite gouge samples used in this study were collected from Miyakejima Island, Japan, and had an average grain size of 1 μm. To ensure that the same effective pressure was used under both dry and wet conditions, the frictional properties were measured under dry conditions at a confining pressure of 150 MPa, and under wet conditions at a confining pressure of 200 MPa and a pore-water pressure of 50 MPa. Temperature was controlled by the outputs from two thermocouples, one at the top and the other at the bottom of the sample (Table 1). The apparatus and experimental procedure are described in more detail in Masuda et al. (2019).

The dependence of friction on velocity was measured by changing the axial displacement rate of the loading piston from 0.5 to 5.0 μm/s after steady-state strengthening was reached. The displacement of the loading piston was measured by a linear variable differential transformer located outside the pressure vessel, and the force applied to the sample was measured by two load cells, one attached outside and the other inside the pressure vessel. To calculate the frictional properties of the samples, internal load cell data were used when they were available; in other cases, external load cell data were used after correction for the friction due to the O-ring used as the seal between the loading piston and the pressure vessel (Noda and Takahashi 2016). The friction coefficient μ is defined as the ratio of shear stress τ to normal stress σ_n on the sliding surface (Eq. 1), and the velocity dependence of steady-state friction ($a - b$) is defined as the ratio of the change in steady-state friction μ_{ss} to the change of slip velocity V (Eq. 2): **see formulas 1 and 2 in the supplementary files.**

where σ_{diff} is the differential stress in the loading direction, q is the angle between the sliding surface and the loading direction (30° in this study), and P_c is the effective confining pressure (150 MPa). The velocity dependence of steady-state friction ($a - b$) is thus estimated as the difference between the parallel trends of steady-state friction before and after the velocity changes. In those cases in which the samples showed stick-slip behavior, the trend of the frictional curve was determined as the slope estimated by using the lowest points in each stick-slip cycle. Laboratory studies have shown that the mechanism of earthquake nucleation is controlled by the frictional properties of materials (e.g. Scholz, 1998; Marone 1998). Because the focus of this study was on the potential of crustal materials for earthquake nucleation at the very beginning of fault movement, whether the frictional properties of the materials were seismic or aseismic was evaluated based on whether the parameter ($a - b$) was positive or negative. If ($a - b$) > 0, the material is considered velocity strengthening and is stable, corresponding to aseismic conditions. If ($a - b$) < 0, the material is considered velocity weakening and is unstable, corresponding to conditions in a seismogenic zone (Scholz 1998, 2019).

Results

Examination of the friction coefficient μ as a function of the displacement of the loading piston (Fig. 1) showed that with a displacement rate of 0.5 μm/s, steady-state strengthening occurred when displacement was around 2 mm and μ = 0.64–0.75 (average 0.69; Table 1). To measure the velocity dependence of friction, when the displacement was around 2 mm, the displacement rate was abruptly increased from 0.5 to 5.0 μm/s (fast step) (Dieterich 1979, 1981, 2009; Scholz 1998), and in some runs, the sliding velocity was changed from 5.0 to 0.5 μm/s (slow step) after the fast step. ($a - b$) was calculated from the portion of the curve before and after the fast step (Fig. 2 and Table 1). Under dry conditions at temperatures up to 400 °C, ($a - b$) of anorthite was positive, whereas at 500 and 600 °C, ($a - b$) was negative. Thus, in the dry state, anorthite was unstable at higher temperatures (Fig. 2a). Under wet conditions at 200 °C, ($a - b$) was negative (Fig. 2b), and the friction versus displacement curve showed stick–slip behavior both before and after the velocity step. ($a - b$) was also negative at 400 °C, but the curve showed stick–slip behavior only after the velocity step (Fig. 1c). In contrast, Masuda et al. (2019) did not observe stick–slip behavior in their experiments with albite samples.

Discussion

Masuda et al. (2019) conducted laboratory experiments with quartz and albite and reported that feldspar plays a more dominant role than quartz in limiting the depth extent (thickness) of the seismogenic zone, but the frictional behaviors of other minerals in the lower seismogenic zone still need to be characterized. Frictional behavior depends in part on environmental conditions, including temperature and the presence of water (Blanpied et al. 1995; Scholz 1998), and the heterogeneity of fault materials (Barnes et al. 2020) or surface morphology (Kirkpatrick et al, 2020) at the interface between seismic and aseismic zones also affects seismogenic processes. Therefore, it is important to know the physical properties, especially the frictional properties, of materials in the transition zone around this interface to better understand

seismogenic mechanisms. Recent advances in seismological observation and analysis techniques have allowed seismic velocity and density distributions to be determined in detail, but information on the physical properties of materials in high-seismicity regions is still lacking. Only laboratory measurements can provide basic physical information about materials, such as their frictional stability.

Effect of water on the frictional characteristics of materials

The velocity dependence of friction ($a - b$) of quartz and feldspar, the two main components of the Earth's crust, is mostly positive under dry conditions at temperatures corresponding to those in fault zones (Masuda et al. 2019; Fig. 2a). Under wet conditions, however, ($a - b$) is negative at temperatures of 200–400 °C. These results are similar to those observed in experiments using granite gouge, a main component of crustal rocks (Lockner et al. 1986; Blanpied et al. 1995). These experimental findings suggest that seismic behavior is induced in the deep crust in the presence of water. Various studies have shown that the mechanism by which water affects frictional behavior in the deep crust is solution-precipitation-aided cataclastic flow (e.g., Blanpied et al. 1995; Masuda et al. 2019). Here, scanning electron microscope images of anorthite gouge samples after the experiments showed rounded grains only after the experiments conducted under wet conditions (Additional file 1). This result suggests that pressure solution occurred in the experiments under wet conditions.

Compared with quartz, plagioclase feldspars (albite and anorthite) have negative ($a - b$) values over a wider temperature range. This result suggests that under wet conditions, the frictional characteristics of feldspar minerals play an important role in limiting the depth extent of the seismogenic zone. The results of our anorthite experiments (Fig. 2) support the results of the albite experiments conducted by Masuda et al. (2019). Moreover, unlike albite, anorthite showed stick–slip behavior under wet conditions at temperatures of 200 and 400 °C. In geologic materials, stick–slip behavior is associated with brittle deformation such as slip on a fault (e.g., Brace and Byerlee 1966). This observed brittle behavior thus suggests that the frictional characteristics of anorthite can account for fault movements in the brittle–plastic transition region.

Lower boundary of the seismogenic zone

Mechanically weak heterogeneities at the base of the seismogenic zone would localize deformation in the brittle–plastic transition region and cause brittle faulting. The physical properties of anorthite support this concept. The stick–slip behavior observed in anorthite ($CaAl_2Si_2O_8$) was not observed in albite ($NaAlSi_3O_8$) (Masuda et al. 2019). Under ambient conditions, the feldspar mineral structure is based on TO_4 tetrahedra (where T = Si^{4+} or Al^{3+}), within which low-charge cations (Na^+ or Ca^+) occupy large voids. Commonly, feldspars are thermodynamically stable at pressures up to 3 GPa. Because TO_4 tetrahedra show very little compression, they behave as a relatively rigid unit (e.g., Pakhomova et al. 2020). This rigidity may be one reason that feldspar is associated with brittle sliding even at high temperatures. In addition, because Ca^+ is heavier than Na^+, anorthite, the calcic endmember of the series, may be more rigid and therefore exhibit more brittle behavior (such as stick–slip behavior) than albite. In field

observations of an exhumed fault zone exposed along the Hatagawa Fault Zone, northeast Japan, many localized brittle deformation zones, including highly fractured crush zones, are observed. In these zones, numerous fractures may have nucleated by fracturing of highly deformed fine-grained feldspar (Shigematsu et al. 2009).

In this study, we investigated anorthite, one mineral component of the Earth's crust. However, measurements of many component minerals and composite materials under a wide variety of possible conditions, as well as laboratory measurements of materials obtained by deep drilling projects (e.g., Kirkpatrick et al. 2020), are needed to construct a reliable conceptual model of seismic processes in the brittle–plastic transition zone at the depth limit of the seismogenic zone.

Declarations

Ethics approval and consent to participate

Not applicable

Consent for publication

Not applicable

List of abbreviations

Not applicable

Availability of data and materials

Tables of the data used to plot the friction curves in Fig. 1 are available as Additional file 2 in the Supplemental information.

Competing interests

The author declares that he has no competing interests.

Funding

This work was supported by the general managing fund from the Geological Survey of Japan, National Institute of Advanced Industrial Science and Technology (AIST).

Author’s contributions

KM designed the study, conducted the experiments, analyzed the data, and prepared the manuscript.

Acknowledgements

Takashi Arai and Miki Takahashi contributed to the experiments by collecting data on frictional characteristics. Yasuko Okuyama provided the anorthite gouge samples for this study. The manuscript has been edited carefully by two native-English-speaking professional editors from ELSS, Inc. The constructive reviews of two anonymous reviewers were very helpful in improving the manuscript.

Authors' information

N/A

Endnotes

None

References

1. Barnes PM, Wallace LM, Saffer DM, Bell RE, Underwood MB, Fagereng A, Meneghini F, Savage HM, Rabinowitz HS, Morgan JK, Kitajima H, Kutterolf S, Hashimoto Y, Engelmann de Oliveira CH, Noda A, Crundwell MP, Shepherd CL, Woodhouse AD, Harris RN, Wang M, Henrys S, Barker DH, Petronotis KE, Bourlange SM, Clennell MB, Cook AE, Dugan BE, Elger J, Fulton PM, Gamboa D, Greve A, Han S, Hüpers A, Ikari MJ, Ito Y, Kim GY, Koge H, Lee H, Li X, Luo M, Malie PR, Moore GF, Mountjoy JJ, McNamara DD, Paganoni M, Screaton EJ, Shankar U, Shreedharan S, Solomon EA, Wang X, Wu H -Y, Pecher IA, LeVay LJ, IODP Expedition 372 Scientists (2020) Slow slip source characterized by lithological and geometric heterogeneity. Science Advances 6, eaay3314. doi: 10.1126/sciadv.aay3314
2. Blanpied ML, Lockner DA, Byerlee JD (1991) Fault stability inferred from granite sliding experiments at hydrothermal conditions. Geophysical Research Letters 18:609–612. doi:10.1029/91GL00469.
3. Blanpied ML, Lockner DA, Byerlee JD (1995) Frictional slip of granite at hydrothermal conditions. Journal of Geophysical Research 100:13045–13064. doi:10.1029/95JB00862
4. Brace WF, Byerlee JD (1966) Stick-Slip as a Mechanism for Earthquakes. Science 153 (3739), 990-992. doi: 10.1126/science.153.3739.990
5. Chester FM, Higgs NG (1992) Multimechanism friction constitutive model for ultrafine quartz gouge at hypocentral conditions. Journal of Geophysical Research 97:1859-1870. doi:10.1029/91JB02349.
6. Dieterich JH (1979) Modeling of rock friction: 1. Experimental results and constitutive equations. Journal of Geophysical Research 84:2161-2168. doi:10.1029/JB084iB05p02161
7. Dieterich JH (1981) Constitutive properties of faults with simulated gouge. In: Carter NL, Friedman M, Logan JM, Stearns DW (Eds.) Mechanical behavior of crustal rocks. The Handin Volume, Geophysical Monograph Series (Vol. 24, pp. 103-120), Washington DC: American Geophysical Union. doi:10.1029/GM024
8. Dieterich JH (2009) Applications of rate- and state-dependent friction to models of fault slip and earthquake occurrence. In: Kanamori H (Ed.) Earthquake Seismology, Treatise on Geophysics, (Vol. 4,

pp. 107-129), Netherlands: Elsevier. doi:10.1016/B978-0-444-53802-4.00075-0

9. Hasegawa A, Yamamoto A (1994) Deep, low-frequency microearthquakes in or around seismic low-velocity zones beneath active volcanoes in northeastern Japan. Tectonophysics 233:233-252. doi:10.1016/0040-1951(94)90243-7.
10. Kirkpatrick JD, Edwards JH, Verdecchia A, Kluesner JW, Harrington RM, Silver EA (2020) Subduction megathrust heterogeneity characterized from 3D seismic data, Nature Geoscience 13: 369–374. doi.org/10.1038/s41561-020-0562-9
11. Lockner DA, Summers R, Byerlee JD (1986) Effects of temperature and sliding rate on frictional strength of granite. Pure and Applied Geophysics 124:445-469. doi:10.1007/BF00877211
12. Marone C (1998) Laboratory-derived friction laws and their application to seismic faulting. Annual Review of Earth and Planetary Science 26: 643-696. doi:10.1146/annurev.earth.26.1.643.
13. Masuda K, Fujimoto K, Arai T (2002) A new gas-medium, high-pressure and high –temperature deformation apparatus at AIST, Japan. Earth, Planets and Space 54(11): 1091–1094. doi:10.1186/BF03353307
14. Masuda K, Iryo K, Ogura A (2006) Internal furnace for the gas-medium high-pressure and high-temperature apparatus at the Geological Survey of Japan/AIST. Japanese Journal of Structural Geology 49:73-76
15. Masuda K, Arai T, Takahashi M (2019) Effects of frictional properties of quartz and feldspar in the crust on the depth extent of the seismogenic zone. Progress in Earth and Planetary Science 6:50. doi: 10.1186/s40645-019-0299-5
16. Noda H, Takahashi M (2016) Correction of output from an internal load cell in a high-pressure triaxial deformation apparatus without a split-piston. Journal of Geological Society of Japan 122(12): 653-658. doi:10.5575/geosoc.2016.0047
17. Pakhomova A, Simonova D, Koemets I, Koemets E, Aprilis G, Bykov M, Gorelova L, Fedotenko T, Prakapenka V, Dubrovinsky L (2020) Polymorphism of feldspars above 10 GPa. Nature Communications 11:2721. doi.org/10.1038/s41467-020-16547-4
18. Scholz CH (1998) Earthquakes and friction laws. Nature 391:37-42. doi:10.1038/34097
19. Scholz CH (2019) The mechanics of earthquakes and faulting, 3rd ed., Cambridge University Press. Cambridge. doi:10.1017/9781316681473
20. Shigematsu N, Fujimoto K, Ohtani T, Shibazaki B, Tomita T, Tanaka H, Miyashita Y (2009) Localisation of plastic flow in the mid-crust along a crustal-scale fault: Insight from the Hatagawa Fault Zone, NE Japan. Journal of Structural Geology 31(6), 601-614. doi.org/10.1016/j.jsg.2009.04.004
21. Takahashi M, Mizoguchi K, Kitamura K, Masuda K (2007) Effects of clay content on the frictional strength and fluid transport property of faults. Journal of Geophysical Research 112:B8, B08206. doi:10.1029/2006JB004678
22. Takahashi M, Uehara S, Mizoguchi K, Shimizu I, Okazaki K, Masuda K (2011) On the transient response of serpentine (antigorite) gouge to stepwise changes in slip velocity under high-temperature

conditions. Journal of Geophysical Research 116: B10405. doi:10.1029/2010JB008062

Table

Due to technical limitations, the table can only be accessed as a download in the supplementary files section.

Figures

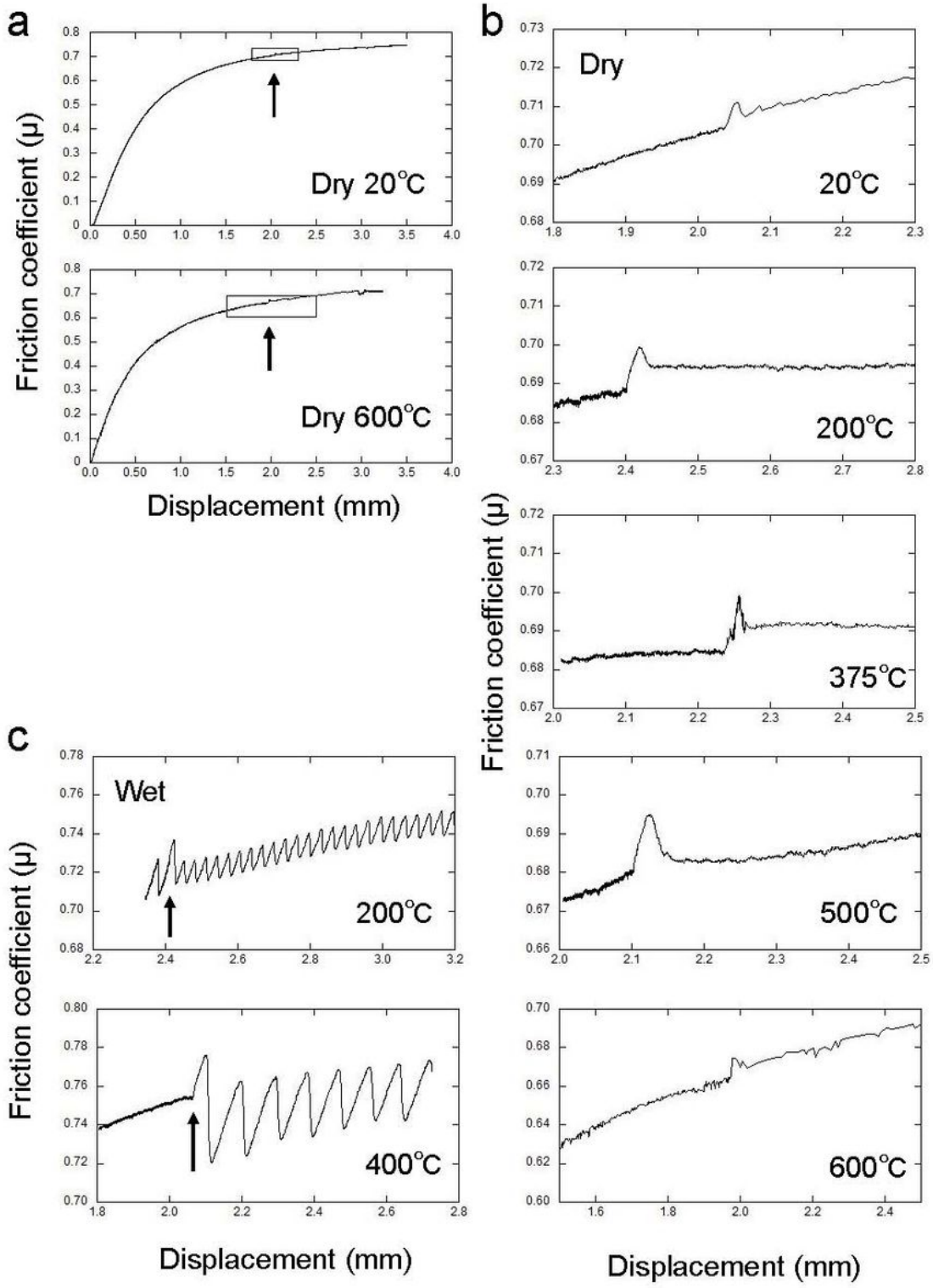

Figure 1

Friction curves obtained in the experiments on anorthite. The friction coefficient μ, as defined in Eq. (1), is plotted as a function of the displacement of the loading piston. a Dry samples at 20 and 600 °C. The boxes show the portion of the curves enlarged in b. The part of the friction curve around the velocity steps: b dry samples at 20, 200, 375, 500, and 600 °C; c wet samples at 200 and 400 °C. The arrows in a and c indicate the timing of the fast step in sliding velocity.

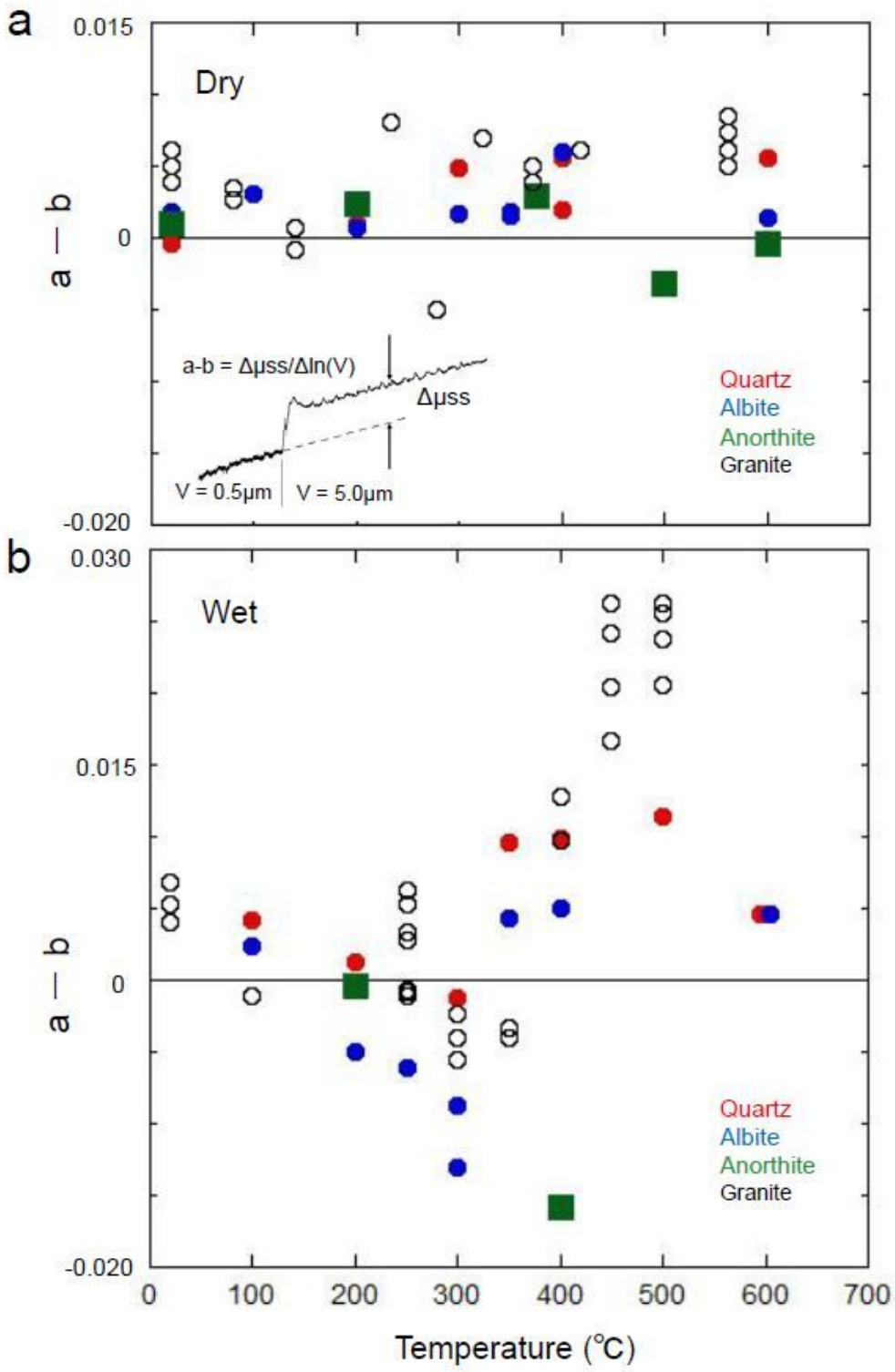

Figure 2

Velocity dependence of steady-state friction (a – b) for anorthite, albite, and quartz, as determined by Eq. (2). a Dry conditions, Pc = 150 MPa (Ar gas); b wet conditions, Pc = 200 MPa (Ar gas), Pp (pore-water pressure) = 50 MPa (distilled water). The data for quartz and albite are from Masuda et al. (2019). The granite data for dry and wet conditions are from Lockner et al. (1986) and Blanpied et al. (1991), respectively. The velocity dependence of steady-state friction (a – b), as determined from eq. (2), is

represented by the difference between the parallel steady-state trend lines immediately before and after velocity step changes (inset diagram in a).

Supplementary Files

This is a list of supplementary files associated with this preprint. Click to download.

- formulas.docx
- Table1.xlsx
- GAI.jpg
- TableS1.xlsx
- FigureS1.jpg